TECHNISCHE MECHANIK, 30, 1-3, (2010), 146 – 156
submitted: October 31, 2009

Characterization of micro-mechanical deformation systems of magnesium based on energy minimization

M. Homayonifar, J. Mosler

The present paper is concerned with a variationally consistent approach suitable for the modeling of rate-independent crystal plasticity at finite strains including a Taylor-type phase transition. The method relies strongly on the variational structure of crystal plasticity theory, i.e., an incremental minimization principle can be derived in case of a fully associative model which allows to compute the unknown slip rates by computing the respective stationarity conditions. More precisely, all internal variables are obtained by minimizing the stress power. For modeling twinning, which is the second important physical process governing the deformation behavior of magnesium, a simple approach for phase transition based on volume averaging is proposed. In line with the modeling of the plastic slip, the proposed method is fully variational, i.e., phase transformation occurs, if this is energetically favorable. Comparisons of numerical results predicted by the novel model to experimental results show that the Taylor-type phase transition is able to capture the hardening transition corresponding to the initial and the twin phase realistically. The same can be observed for the hardening behavior of ordinary dislocation systems of magnesium characterized by means of the channel die test.

1 Introduction

Light-weight materials are of great importance in many different industries. For instance, in the transportation industry, those materials can be used to efficiently reduce fuel consumption and thus, the green house gas emissions. One very promising lightweight material is magnesium and its alloys. Due to its high specific strength and its relatively low cost, it challenges aluminum alloys in some applications such as those in automotive industries. The deformation behavior of magnesium is defined by its hexagonal crystal structure. It leads to a limited number of dislocation systems and consequently, twinning is a common structural deformation response. Investigations on the plastic deformation systems of magnesium have been originated by early studies of dislocations and twinning in hexagonal materials, see (Schmid, 1924; Siebel, 1939). Since then, experimental observations have revealed that more deformation systems can be activated under different boundary conditions, see (Hauser et al., 1955; Reed-Hill and Robertson, 1957b; Yoshinaga and Horiuchi, 1963; Tegart, 1964; Wonsiewicz and Backofen, 1967; Roberts and Partridge, 1966; Obara et al., 1973; Ando and Tonda, 2000). Concerning the modeling approaches for magnesium and its alloys, the majority of those models is based on polycrystal plasticity approaches, see(Lebensohn and Tom, 1993; Agnew et al., 2001; Agnew and Duygulu, 2003; Beausir and Suwas, 2008). For instance, Beaudoin et al. proposed a hybrid formulation to combine the polycrystal plasticity theory with the finite element method, in order to model the non-uniform deformation of crystalline solids (Beaudoin et al., 1995; Kumar and Dawson, 1998; Myagchilov and Dawson, 1999). Recently, this method has been used to analyze the plastic effects in magnesium alloys under more complicated boundary conditions such as those related to cup drawing, see Tang et al. (2009). Most of the aforementioned models fall into the range of crystal plasticity theory. Although rate-independent and rate-dependent crystal plasticity are relatively well understood from a physical point of view, cf. Asaro (1983), many problems are still open. One example is given by the computation of the active slip systems in magnesium, which can be an ill-conditioned problem. Possible solutions are an explicit integration scheme, see Graff et al. (2007), or a modified algorithmic method as proposed in (Miehe and J. Schroeder, 2001; Staroselsky and Anand, 2003; McGinty and McDowell, 2006). Within the present paper, the aforementioned problem is naturally solved by elaborating a so-called *variational constitutive update*, cf. (Ortiz and Repetto, 1999; Ortiz et al., 2000; Carstensen et al., 2002; Lambrecht et al., 2003; Bartels et al., 2004; Ortiz and Repetto, 1999; Mosler and Bruhns, 2009a,b). In contrast to conventional schemes, variational updates allow to compute the unknown slip deformations by minimizing a certain energy. Thus, they automatically and naturally define the set of active slip planes by energy minimization. Furthermore, they permit to analyze other important physical phenomena in crystals. For instance, such formulations reveal that the linear dependency of dislocation slips and the latent hardening may yield a non-

convex energy and hence, they are related to an evolving sub-grain micro-structure, see Ortiz and Repetto (1999).

In the present paper, a fully variational description of the deformation systems in magnesium is discussed. In addition to plastic slip, it also covers deformation-induced twinning. This phase transformation is modeled fully analogously to that observed in shape memory alloys, see Mielke (2004). More precisely, starting with a mixture theory, a re-orientation associated with twinning occurs, if this is energetically favorable. The resulting variationally consistent implementation of the incremental energy minimization concept for modeling of magnesium single crystal is critically analyzed by comparing the numerically predicted results to experiments.

2 Fundamentals of finite strain plasticity theory

In this section, the fundamentals of finite strain plasticity theory are briefly summarized. This section serves mainly for introducing the notations used in this paper. As usual, the deformation of a solid $\Omega \subset \mathbb{R}^3$ is defined by the deformation mapping $\boldsymbol{\varphi}(\boldsymbol{X}) : \Omega \to \mathbb{R}^3$. For modeling inelastic processes such as those related to plastic slip, a multiplicative decomposition of the deformation gradient $\boldsymbol{F} = \mathrm{GRAD}\boldsymbol{\varphi}(\boldsymbol{X})$ into a plastic part $\boldsymbol{F}^{\mathrm{p}}$, which transforms the reference body into a stress free intermediate configuration, and an elastic part $\boldsymbol{F}^{\mathrm{e}}$ corresponding to the elastic distortion is assumed (see Lee (1969)), i.e.,

$$\boldsymbol{F} = \boldsymbol{F}^{\mathrm{e}} \cdot \boldsymbol{F}^{\mathrm{p}} \ , \ \text{with} \ \det(\boldsymbol{F}^{\mathrm{e}}) > 0 \ , \ \det(\boldsymbol{F}^{\mathrm{p}}) > 0. \tag{1}$$

In order to describe the history of plastic deformations of the solid, a finite set of strain-like internal variables $\boldsymbol{\alpha} \subset \mathbb{R}^n$ is introduced, Lubliner (1972). Based on these variables, together with the decomposition (1), the Helmholtz energy for an isothermal process is postulated as

$$\Psi = \Psi(\boldsymbol{F}^{\mathrm{e}}, \boldsymbol{\alpha}), \tag{2}$$

(Lubliner, 1972, 1997; Simo and Hughes, 1998). Since the elastic stored energy depends only on the elastic distortion, the Helmholtz energy can be decomposed additively into Ψ^{e} for the elastic part and Ψ^{p} corresponding to the plastic work. Combining this with the principle of material frame indifference, the total stored energy can thus be written as

$$\Psi = \Psi^{\mathrm{e}}(\boldsymbol{C}^{\mathrm{e}}) + \Psi^{\mathrm{p}}(\boldsymbol{\alpha}) \ , \ \boldsymbol{C}^{\mathrm{e}} := \boldsymbol{F}^{\mathrm{e}^{\mathrm{T}}} \cdot \boldsymbol{F}^{\mathrm{e}} \tag{3}$$

where $\boldsymbol{C}^{\mathrm{e}}$ is the right Cauchy-Green tensor. Irreversible processes, in particular plastic deformations, are entropy productive processes and consequently, they have to fulfill the second law of the thermodynamics. For that purpose, the evolution equations for the irreversible plastic process are obtained by using the Clausius-Planck dissipation inequality (see Coleman (1964)), i.e.,

$$\mathcal{D} = \boldsymbol{P} : \dot{\boldsymbol{F}} - \dot{\Psi} = \boldsymbol{S} : \frac{1}{2}\dot{\boldsymbol{C}} - \dot{\Psi} \geq 0. \tag{4}$$

Here, $\boldsymbol{P}$ is the first Piola-Kirchhoff stress tensor, $\boldsymbol{S}$ is the second Piola-Kirchhoff stress tensor and the superimposed dot represents the material time derivative. Applying the Coleman & Noll procedure for an elastic unloading step yields the classical elastic response

$$\boldsymbol{S} = 2\frac{\partial \Psi}{\partial \boldsymbol{C}} = 2(\boldsymbol{F}^{\mathrm{p}})^{-1} \cdot \frac{\partial \Psi}{\partial \boldsymbol{C}^{\mathrm{e}}} \cdot (\boldsymbol{F}^{\mathrm{p}})^{-\mathrm{T}} \tag{5}$$

Inserting this equation into the dissipation inequality, together with the definition of the stress-like internal variable

$$\boldsymbol{Q} = -\frac{\partial \Psi}{\partial \boldsymbol{\alpha}} \tag{6}$$

being thermodynamically conjugate to the strain-like internal variable $\boldsymbol{\alpha}$, the reduced dissipation inequality

$$\mathcal{D} = \boldsymbol{\Sigma} : \boldsymbol{L}^{\mathrm{p}} + \boldsymbol{Q} \cdot \dot{\boldsymbol{\alpha}} \geq 0 \tag{7}$$

can be derived. Here, the Mandel stresses $\boldsymbol{\Sigma} = 2\boldsymbol{C}^{\mathrm{e}} \cdot \partial_{\boldsymbol{C}^{\mathrm{e}}} \Psi$ (see Mandel (1972)) and the plastic velocity gradient $\boldsymbol{L}^{\mathrm{p}} = \dot{\boldsymbol{F}}^{\mathrm{p}} \cdot (\boldsymbol{F}^{\mathrm{p}})^{-1}$ have been used.

For differentiating between elastic unloading and plastic loading, an admissible stress space $\mathbb{E}_{\boldsymbol{\sigma}}$ of the type

$$\mathbb{E}_{\boldsymbol{\sigma}} = \left\{ (\boldsymbol{\Sigma}, \boldsymbol{Q}) \in \mathbb{R}^{9+n} \;\middle|\; \phi(\boldsymbol{\Sigma}, \boldsymbol{Q}) \leq 0 \right\} \tag{8}$$

is introduced, see Lubliner (1972). Here, ϕ is a convex yield function. The material is postulated to be in a purely elastic state, if $(\boldsymbol{\Sigma}, \boldsymbol{Q}) \in \text{int}\, \mathbb{E}_{\boldsymbol{\sigma}}$, while for $(\boldsymbol{\Sigma}, \boldsymbol{Q}) \in \partial \mathbb{E}_{\boldsymbol{\sigma}}$ plastic deformation are possible (only necessary condition). In what follows, yield functions of the type

$$\phi(\boldsymbol{\Sigma}, \boldsymbol{Q}) = \Sigma_{\text{eq}}(\boldsymbol{\Sigma}, \boldsymbol{Q}) - \Sigma_{\text{eq}}^{\text{ini}} \tag{9}$$

are considered. Here, Σ_{eq} is an equivalent stress measure defining the shape of the elastic domain and $\Sigma_{\text{eq}}^{\text{ini}} > 0$ specifies its initial diameter.

Evolution equations can be naturally obtained from the postulate of maximum dissipation. More precisely, in this case, they are given by

$$\boldsymbol{L}^{\text{p}} = \dot{\lambda} \frac{\partial \phi}{\partial \boldsymbol{\Sigma}} \;,\; \dot{\boldsymbol{\alpha}} = \dot{\lambda} \frac{\partial \phi}{\partial \boldsymbol{Q}}, \tag{10}$$

together with the Karush-Kuhn-Tucker optimality conditions (see Luenberger (1984))

$$\dot{\lambda} \geq 0 \;,\; \dot{\lambda}\, \dot{\phi} \geq 0. \tag{11}$$

In those equations, $\dot{\lambda}$ is the plastic multiplier which can be obtained from the consistency condition $\dot{\phi} = 0$. Eq. (10) shows that the rate of internal variables and the velocity gradient are proportional to the gradient of the yield function which is also known as normality rule.

3 Single Crystal Plasticity

Plastic deformations in metallic materials can be modeled by the plastic slip caused by dislocations. The resultant shear strain of the dislocation movement can be characterized by two orthogonal unit vectors $\boldsymbol{m}$ and $\boldsymbol{s}$ which correspond to the normal of the plane and the direction of the plastic shear, respectively. Classical crystal plasticity is usually based on an associative flow rule resulting from Schmid's law. This law is defined by a yield function of the type

$$\phi^a(\boldsymbol{\Sigma}, \lambda^a) = \Sigma_{\text{eq}}^a(\boldsymbol{\Sigma}, Q) - \Sigma_{\text{ini}}^a = |\boldsymbol{\Sigma} : \boldsymbol{N}^a| - Q^a(\lambda^a) - \Sigma_{\text{ini}}^a \tag{12}$$

where λ^a is the accumulated plastic shear strain, Q^a represents an internal stress-like variable associated with isotropic hardening and Σ_{ini}^a corresponds to the critical resolved shear stress of the ath dislocation system. The driving force for the dislocation glide, the so-called Schmid stress, is obtained by the projection of the applied stress $\boldsymbol{\Sigma}$ using the Schmid tensor $\boldsymbol{N}^a = (\boldsymbol{s}^a \otimes \boldsymbol{m}^a)$. The admissible stress space $\tilde{\mathbb{E}}_{\boldsymbol{\sigma}}$ for the single crystal is defined by the intersection of all single surfaces, i.e.,

$$\tilde{\mathbb{E}}_{\boldsymbol{\sigma}} = \left\{ (\boldsymbol{\Sigma}, \boldsymbol{Q}) \in \mathbb{R}^{9+n} \;\middle|\; \phi^a(\boldsymbol{\Sigma}, Q^a) \leq 0,\; a = 1, ..., n \right\}. \tag{13}$$

Following Eq. (10), evolution equations of the internal variables related to dislocation slip are derived from the principle of maximum dissipation yielding

$$\boldsymbol{L}^{\text{p}} = \sum_{a=1}^{n} \dot{\gamma}^a \boldsymbol{N}^a \;,\; \dot{\gamma}^a = \dot{\lambda} \cdot \text{sign}[\boldsymbol{\Sigma} : \boldsymbol{N}^a], \;\; \dot{\lambda}^a \geq 0 \tag{14}$$

By inserting Eq. (14) into the dissipation inequality Eq. (7) and considering that the equivalent stresses are positively homogeneous of degree one, i.e.,

$$\Sigma_{\text{eq}}^a(c\boldsymbol{\Sigma}, cQ^a) = c\, \Sigma_{\text{eq}}^a(\boldsymbol{\Sigma}, Q^a) \;,\; \forall c \in \boldsymbol{R}_+ \tag{15}$$

the dissipation with respect to a single dislocation slip reduces to

$$\mathcal{D}^a = \dot{\lambda}^a \cdot \text{sign}[\boldsymbol{\Sigma} : \boldsymbol{N}^a](\boldsymbol{\Sigma} : \boldsymbol{N}^a) - \dot{\lambda}^a (Q_{\mathbf{se}}^a + Q_{\mathbf{le}}^{ab}) \overset{\phi^a = 0}{=} \dot{\lambda}^a \cdot \Sigma_{\text{ini}}^a \geq 0. \tag{16}$$

Since both terms are positive, the second law of thermodynamics is indeed fulfilled. The total plastic dissipation with respect to the n dislocation is given by

$$\mathcal{D} = \sum_{a=1}^{n} \mathcal{D}^a \geq 0. \tag{17}$$

4 The variational structure of single crystal plasticity theory

In this section, the crystal plasticity model briefly discussed in the previous section is recast into a variational framework. Within this framework, every physical aspect is consistently driven by energy minimization. For the sake of simplicity, the underlying idea is explained by considering only one active slip plane (one yield function). However, the method can be extended to multiple dislocations systems in a straightforward manner. Following (Ortiz, 1999; Mosler and Bruhns, 2009b), the functional

$$\tilde{\mathcal{E}}(\dot{\boldsymbol{\varphi}}, \dot{\boldsymbol{F}}^{\mathrm{p}}, \dot{\lambda}, \boldsymbol{\Sigma}, \boldsymbol{Q}) = \dot{\Psi}(\dot{\boldsymbol{\varphi}}, \dot{\boldsymbol{F}}^{\mathrm{p}}, \dot{\lambda}) + \mathcal{D}(\dot{\boldsymbol{F}}^{\mathrm{p}}, \dot{\lambda}, \boldsymbol{\Sigma}, \boldsymbol{Q}) + J(\boldsymbol{\Sigma}, \boldsymbol{Q}) \tag{18}$$

is introduced, where $J(\boldsymbol{\Sigma}, \boldsymbol{Q})$ is the characteristic function of the admissible stress state, i.e.,

$$J := \begin{cases} 0 & \forall (\boldsymbol{\Sigma}, \boldsymbol{Q}) \in \mathbb{E}_\sigma \\ \infty & \text{otherwise.} \end{cases} \tag{19}$$

Accordingly, J penalizes the functional (18) for inadmissible stress states. For admissible stress states, i.e. $(\boldsymbol{\Sigma}, \boldsymbol{Q}) \in \mathbb{E}_\sigma$, the functional reduces to the sum of the rate of the Helmholtz energy and the dissipation. Consequently, the functional $\tilde{\mathcal{E}}$ equals the stress power $\mathcal{P}$, i.e.,

$$\tilde{\mathcal{E}}(\dot{\boldsymbol{\varphi}}, \dot{\boldsymbol{F}}^{\mathrm{p}}, \dot{\lambda}, \boldsymbol{\Sigma}, \boldsymbol{Q}) = \boldsymbol{P} : \dot{\boldsymbol{F}} =: \mathcal{P}, \quad \forall (\boldsymbol{\Sigma}, \boldsymbol{Q}) \in \mathbb{E}_\sigma. \tag{20}$$

It can be shown that the stationarity condition of functional (18) is equivalent to the crystal plasticity model discussed in the previous section. Hence, it represents a variational re-formulation. This variational method can be transformed into a minimization problem, if a maximization with respect to the stress-like variables is performed. Physically speaking, this is equivalent to enforcing the principle of maximum dissipation. This leads to the reduced functional

$$\mathcal{E}(\dot{\boldsymbol{\varphi}}, \dot{\boldsymbol{F}}^{\mathrm{p}}, \dot{\lambda}) = \dot{\Psi}(\dot{\boldsymbol{\varphi}}, \dot{\boldsymbol{F}}^{\mathrm{p}}, \dot{\lambda}) + J^*(\boldsymbol{L}^{\mathrm{p}}, \dot{\lambda}) \tag{21}$$

where J^* is the Legendre transformation of the characteristic function. Physically, it corresponds to the dissipation. Without going too much into details, it can be shown that minimizing functional (21) defines the evolution equations of all internal variables in a canonical manner. More precisely,

$$(\dot{\boldsymbol{F}}^{\mathrm{p}}, \dot{\lambda}) = \arg \inf_{\dot{\boldsymbol{F}}^{\mathrm{p}}, \dot{\lambda}} \mathcal{E}(\dot{\boldsymbol{\varphi}}, \dot{\boldsymbol{F}}^{\mathrm{p}}, \dot{\lambda}). \tag{22}$$

The unknown deformation mapping follows from the same minimization principle. However, since the deformation is defined in a continuous fashion, a global energy minimization is required, i.e.,

$$\boldsymbol{\varphi} = \arg \inf_{\boldsymbol{\varphi}} \boldsymbol{I}_{\mathrm{inc}}(\boldsymbol{\varphi}) \tag{23}$$

with

$$\boldsymbol{I}_{\mathrm{inc}} = \inf_{\boldsymbol{F}^{\mathrm{p}}, \lambda} \left[\int_\Omega \int_{t_n}^{t_{n+1}} \mathcal{E}(\dot{\boldsymbol{\varphi}}, \dot{\boldsymbol{F}}^{\mathrm{p}}, \dot{\lambda}) \, \mathrm{d}t \, \mathrm{d}V - \int_\Omega \rho_0 \boldsymbol{B} \cdot \boldsymbol{\varphi} \, \mathrm{d}V - \int_{\partial\Omega} \boldsymbol{T} \cdot \boldsymbol{\varphi} \, \mathrm{d}A \right] \tag{24}$$

Here, ρ_0, $\boldsymbol{B}$ and $\boldsymbol{T}$ are the material density, body forces and prescribed tractions, respectively. Clearly, for computing the first integral in Eq. (24) a time discretization of the interval $[\Delta t = t_{n+1} - t_n]$ is required. For that purpose, an exponential-type approximation is applied to the evolution equation of $\boldsymbol{F}^{\mathrm{p}}$, while a classical backward-Euler integration is utilized for the plastic slip. Hence,

$$\boldsymbol{F}^{\mathrm{p}}_{n+1} = \exp(\Delta t \boldsymbol{L}^{\mathrm{p}}) \cdot \boldsymbol{F}^{\mathrm{p}}_n \ , \ \lambda^a_{n+1} = \lambda^a_n + \Delta t \cdot \dot{\lambda}^a_{n+1}. \tag{25}$$

Further details are omitted. They can be found, for instance, in Mosler and Bruhns (2009a,b).

5 Multiphase variational formulation

Temperature- and deformation-induced phase transformation are common features observed in a wide range of materials, particularly in metals. Assuming an isothermal process, we focus on the deformation-induced transformation here. For that purpose, the Helmholtz energy associated with a phase mixture is modeled as

$$\Psi(\boldsymbol{C}^{\mathrm{e}}, \boldsymbol{\lambda}, \boldsymbol{\xi}) = \sum_{r=1}^{m} \xi_r \Psi_r(\boldsymbol{C}^{\mathrm{e}}_r, \boldsymbol{\lambda}_r) + \Psi^{\mathrm{mix}}(\xi_r) \ , \quad \Omega := \bigcup_r \Omega_r \tag{26}$$

see (Mielke, 2004; Bartels et al., 2004). The variable $\xi_r \in [0,1]$ defines the volume fraction of the rth phase within the domain Ω_r and $\Psi^{\mathrm{mix}}(\xi_r)$ accounts for an interfacial energy at $\partial\Omega_{\{r_1 r_2\}} := \Omega_{r_1} \cap \Omega_{r_2}$ and $\boldsymbol{\lambda}$ represents the set of internal variables. Considering the Hadamard compatibility condition for the deformation gradient across $\partial\Omega_{\{r_1 r_2\}}$, the elastic strain is defined

$$\boldsymbol{C}^{\mathrm{e}}_{r_2} = (\boldsymbol{F}^{\mathrm{p}}_{r_2})^{-\mathrm{T}} \cdot (\boldsymbol{F}^{\mathrm{T}}_{r_2} \cdot \boldsymbol{F}_{r_2}) \cdot (\boldsymbol{F}^{\mathrm{p}}_{r_2})^{-1} \ , \quad \boldsymbol{F}_{r_2} = \boldsymbol{F}_{r_1} + (\boldsymbol{a}_{\{r_1 r_2\}} \otimes \boldsymbol{n}_{\{r_1 r_2\}}) \tag{27}$$

where $\boldsymbol{n}_{\{r_1 r_2\}}$ and $\boldsymbol{a}_{\{r_1 r_2\}}$ are the normal vector of interface $\partial\Omega_{\{r_1 r_2\}}$ and a vector defining the deformation jump across the interface. Obviously, the vectors $\boldsymbol{a}_{\{r_1 r_2\}}$ cannot be chosen arbitrarily but they have to fulfill a certain compatibility condition. More precisely,

$$\boldsymbol{F} = \sum_{r=1}^{m} \xi_r \boldsymbol{F}_r, \quad \text{with} \quad \sum_{r=1}^{m} \xi_r = 1. \tag{28}$$

Clearly, in case of twinning, only two phases can occur, i.e., $m = 2$. Furthermore, for the sake of simplicity, it is assumed that either the original phase is present or a twin transforms the considered representative volume element completely. With this assumption, a Taylor-type model characterized by

$$\boldsymbol{F} = \xi_{\mathrm{ini}} \boldsymbol{F}_{\mathrm{ini}} + \xi_{\mathrm{Tw}} \boldsymbol{F}_{\mathrm{Tw}} \ , \quad \{\xi_{\mathrm{ini}}, \xi_{\mathrm{Tw}}\} \in \{0,1\} \tag{29}$$

is obtained. $\boldsymbol{F}_{\mathrm{ini}}$ and $\boldsymbol{F}_{\mathrm{Tw}}$ correspond to the deformation gradient in the initial and the twinning phase. In line with the variational method discussed in the previous section, twinning is modeled in a fully variational setting. More precisely, it is assumed that a twin (re-orientation) occurs, if this energetically favorable. For that purpose, the stress power (the incremental energy) of each phase

$$\mathcal{E}(\dot{\boldsymbol{\varphi}}_r, \dot{\boldsymbol{F}}^{\mathrm{p}}_r, \dot{\boldsymbol{\lambda}}_r) = \dot{\Psi}_r(\dot{\boldsymbol{\varphi}}_r, \dot{\boldsymbol{F}}^{\mathrm{p}}_r, \dot{\boldsymbol{\lambda}}_r) + J^*(\boldsymbol{L}^{\mathrm{p}}_r, \dot{\boldsymbol{\lambda}}_r) \tag{30}$$

is considered. Conceptually, this incremental energy is minimized for both configurations (initial orientation of the crystal and reoriented crystal) and the lowest energy signals the physically most likely state. Thus, within this variational method, every physical aspect is consistently driven by energy minimization: the plastic slip as well as twinning.

It bears emphasis that the model can also simulate a continuous transition between the different configurations. For that purpose, the incremental energy characterizing the mixture has also to be minimized with respect the volume fraction ξ_r. Such a method allows to analyze the governing physics at the micro-scale in a more detailed manner. For instance, the influence of the interface energy can be investigated. However, this will certainly increase the numerical cost and thus, the computation time. Since we are mostly interested in the analysis of polycrystals efficiency, is of utmost importance. For this reason, the Taylor-type approximation seems to be more reasonable. Furthermore, as shown in the next section, even this simplified model captures the underlying physics reasonably well.

6 Numerical Example (slip and twinning in magnesium)

The objective of this section is to characterize the deformation systems of magnesium single crystal including twinning. It is well known that twinning is a common deformation observed in a variety of materials, particularly in those showing a hexagonal close packed (HCP) structure. Twinning does not only induce shear strains but also

transforms the crystalline lattice to a new configuration. Consequently, twinning somehow resets the active and inactive slip systems within the twinned domain. As a result, the new configuration may propose new favorable plastic deformations. For analyzing those phenomena, the novel variational method as proposed in the present paper is applied.

We assume that twinning transforms the initial crystal lattice vectors $\boldsymbol{e} := \{\boldsymbol{e}_1, \boldsymbol{e}_2, \boldsymbol{e}_3\}$ to a twinned configuration $\tilde{\boldsymbol{e}}$ by an orthogonal map $\boldsymbol{R}$ with $\det \boldsymbol{R} = 1$, i.e.,

$$\tilde{\boldsymbol{e}} = \boldsymbol{R} \cdot \boldsymbol{e} \tag{31}$$

where $\boldsymbol{R}$ is defined by

$$\boldsymbol{R} = -\boldsymbol{1} + 2(\boldsymbol{n} \otimes \boldsymbol{n}) \tag{32}$$

Here, the normal vector $\boldsymbol{n}$ characterizes the twinning plane. Although the deformation is continuous throughout the total domain, the deformation gradient shows a discontinuity across the twinning boundary (weak discontinuity). More precisely, the deformation gradient within the twin domain $\boldsymbol{F}_{\mathrm{Tw}}$ fulfills a compatibility condition of the type

$$\boldsymbol{F}_{\mathrm{Tw}} = \boldsymbol{F}_{\mathrm{ini}} + (\boldsymbol{a} \otimes \boldsymbol{n}). \tag{33}$$

(see previous section). The basal systems $< 11\bar{2}0 > \{0001\}$ and the prismatic systems $< 11\bar{2}0 > \{\bar{1}100\}$ are mostly responsible for plastic deformation within the HCP crystal. Experimental observations revealed that twinning is the magnesium's major deformation response to loading in the direction of the c-axis. Tensile loading of magnesium single crystal activates twinning at the planes $\{\bar{1}102\}$, while the deformation mode in the opposite loading direction is not clear. Some researcher have observed compression twinning, see Wonsiewicz and Backofen (1967). However, pyramidal slip at the systems $< 11\bar{2}3 > \{11\bar{2}2\}$ has also been reported, see Obara et al. (1973). Tab. 1 summarizes the reported values of the critical resolved shear stresses Σ^a_{ini} for different deformation systems in magnesium. It can be shown that the combination of easy glide (basal dislocations) and tensile twinning with moderate to strong prismatic and pyramidal dislocation systems results in pronounced anisotropic plastic deformations in magnesium single crystal. In order to characterize the aforementioned deformation systems, constrained loading tests were conducted by (Wonsiewicz and Backofen, 1967; Kelley and Hosford, 1968). With help of the channel die test, they applied a plain strain loading on single crystal specimens. More detailed information about the channel die test are omitted here. Different crystal orientations within the channel die result in classes of limited deformation systems. Thus, this test allows to analyze different relatively simple deformation modes separately. For instance, a c-axial compression loading of single crystals activates only a set of pyramidal slip systems. Tab. 2 summarizes the loading and constrained directions of the channel die tests which have been conducted by Kelley and Hosford (1968).

Table 1: Reported critical resolved shear stresses for the deformation systems of magnesium single crystal at room temprature.

	Basal [Mpa]	Prismatic [Mpa]	Pyramidal [Mpa]	Twinning [Mpa]
Burke and Hibbard (1952)	0.45			
Kelley and Hosford (1968)	0.48			
Reed-Hill and Robertson (1957a)				2
Obara et al. (1973)			30-50	
Reed-Hill and Robertson (1957b)		39.3		

Table 2: Definition of the orientations used within the channel die compression test on single crystals Kelley and Hosford (1968)

Test label	Loading direction	Constrained direction
A	$< 0001 >$	$< 10\bar{1}0 >$
C	$< 10\bar{1}0 >$	$< 0001 >$
E	$< 10\bar{1}0 >$	$< 1\bar{2}10 >$
G	$< 0001 >$ at 45^{o}	$< 10\bar{1}0 >$

In order to simplify the twinning problem, we decouple the shear strains and the lattice transformation induced by twinning. More precisely the shear strains of twinning systems are minimized by pseudo-dislocation twinning systems in the initial phase and the lattice transformation is taken into account by a phase decomposition (re-orientation). The elastic response of magnesium is approximated by means of the neo-Hooke-type model

$$\Psi^{\mathrm{e}} = \frac{\lambda_{\mathrm{E}}}{2}(\ln(J))^2 - \mu \ln(J) + \frac{\lambda_{\mathrm{E}}}{2}(\mathrm{tr}(\boldsymbol{C}^{\mathbf{e}}) - 3) \tag{34}$$

where J is the determinant of elastic deformation gradient and $\{\lambda_{\mathrm{E}}, \mu\}$ are Lamé constants. Since the elastic deformations in magnesium are comparatively small, the weak elastic anisotropy and the choice of the elastic material model does not influence the results significantly. The converse is true for the plastic deformations. For this reason, three different plastic stored energies have been implemented. They are related to self-hardening. For the sake of simplicity, linear latent hardening is considered. The different models are summarized below.

$$Q^a_{\mathbf{se}} = \frac{\partial \Psi^{\mathrm{p}}_{\mathbf{se}}}{\partial \lambda^a} = \begin{cases} h_0(\lambda^a) \\ h_0(1 - (\tau_0/\tau_\infty)) \exp(-h_0 \lambda^a/\tau_\infty) \\ h_0(\lambda^a + (\frac{\lambda^a}{\lambda_{\mathrm{crt}}})^n) \end{cases} \tag{35}$$

$$Q^{ab}_{\mathbf{la}} = \frac{\partial^2 \Psi^{\mathrm{p}}_{\mathbf{la}}}{\partial \lambda^a \partial \lambda^b} = l^{ab} \tag{36}$$

The resulting hardening curves are shown in Fig. 1. In order to get a limited shear strain caused by pseudo-dislocation twinning, a ramp-type functions is considered. The exponential and the linear hardening functions characterizing the other deformation modes agree with experimental observations. The boundary value problem describing the channel die test has been solved incrementally, see (Ortiz and Repetto, 1999; Carstensen et al., 2002; Mosler and Bruhns, 2009b). The crystal symmetry and the constrained loading conditions, reduce the number of potentially active slip systems in each sample. The following deformation modes have been analyzed separately:

- Pyramidal dislocations: sample A
- Prismatic slip systems: sample C
- Basal dislocations: sample G
- Pseudo-dislocation twinning: sample E

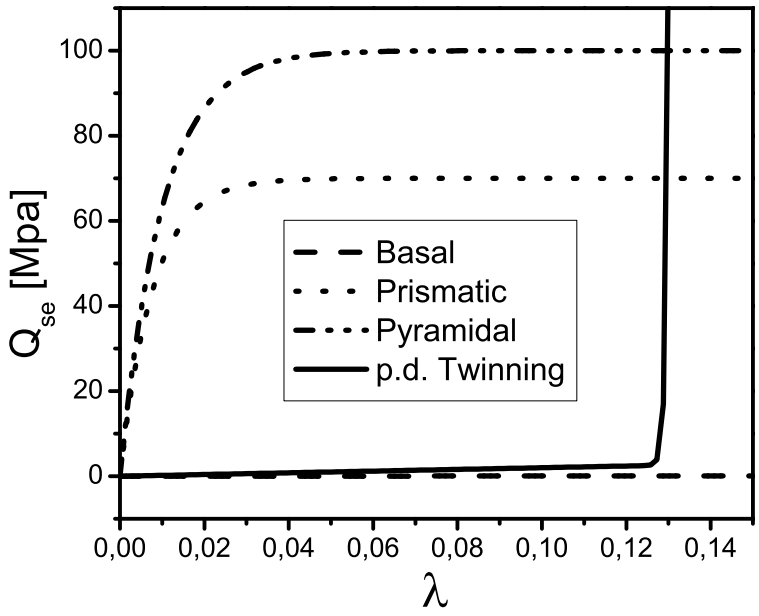

Figure 1: Hardening functions for the different deformation systems of magnesium single crystal

The crystallographic relation between the initial phase and twinning is described by Eq. (31). Experimental x-ray observations revealed that twinning reorients the c-axis of the initial lattice about 86 degrees. Therefore,

pseudo-dislocation twinning is active within the initial phase, while pyramidal slip systems can be observed in the secondary phase. According to the Taylor assumption, the response of the single crystal is solely governed by the phase having the lowest energy (initial or twinned phase). Fig. (2) shows the minima of the incremental energies for both phases. Furthermore, the volume fraction of twinning is included in this diagram as well. Phase transition occurs, if the pseudo- dislocation twinning reaches a certain threshold. This threshold is defined by the respective plastic shear strain λ_{crt}. The second phase corresponding to the reoriented configuration exhibits a strong activity of the pyramidal slip systems. The comparison between the experimental results reported in Kelley and Hosford (1968) and the simulations predicted by the novel variational model in terms of the true stress and the true strain are shown in Fig. 3. Within the computations, the material parameters according to Tab. 3 have been adopted. As evident from Fig. 3, the agreement is excellent.

Table 3: Materials parameters used within the numerical analyses

Elastic Properties	$\lambda_{\mathrm{E}} = 34$(Gpa)			$\mu = 17$ (Gpa)		
Hardening parameters						
	τ_0 (Mpa)	h_0 (Mpa)	τ_∞ (Mpa)	n	λ_{crt}	l^{ab}
Basal	0.48	0.1	-	-	-	0
Prismatic	20	8900	70	-	-	20
Pyramidal	25	7000	100	-	-	25
pseudo-dislocation twinning	2	20	-	100	0.129	10

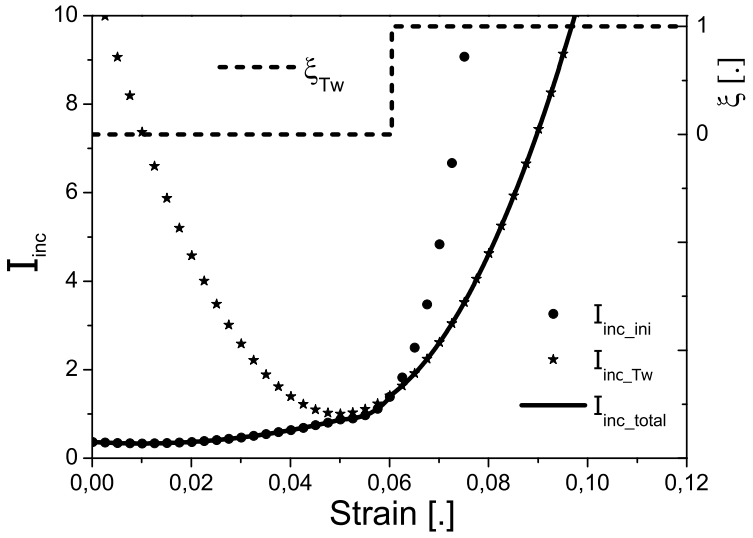

Figure 2: Incremental energy for the initial and the twinning phase as well as the twinning volume fraction for sample E

7 Conclusion

In this paper, a variational constitutive update suitable for the numerical analysis of the deformation behavior of magnesium single crystal was proposed. The novel approach is based on two parts. While the first of those is related to the modeling of plastic slip due to dislocations in crystals, the second part is associated with the simulation of deformation-induced twinning. Concerning plastic slip, a variational method was developed in which every aspect is consistently driven by energy minimization. More precisely, the unknown slip rates follow conveniently from minimizing the stress power. Though the application of variational updates to the modeling of magnesium is new and not straightforward, a similar concept has been already advocated. The opposite is true for the simulation of twinning. While the shear strains related to twinning were taken into account by a pseudo dislocation system, the re-orientation was approximated as a phase transition process. For increasing the efficiency of the proposed model, a Taylor-type theory was adopted. Comparisons between the experimentally observed deformation behavior and the results predicted by the novel model demonstrated an excellent agreement. All physically relevant deformation modes are captured by the model and are driven naturally by energy minimization.

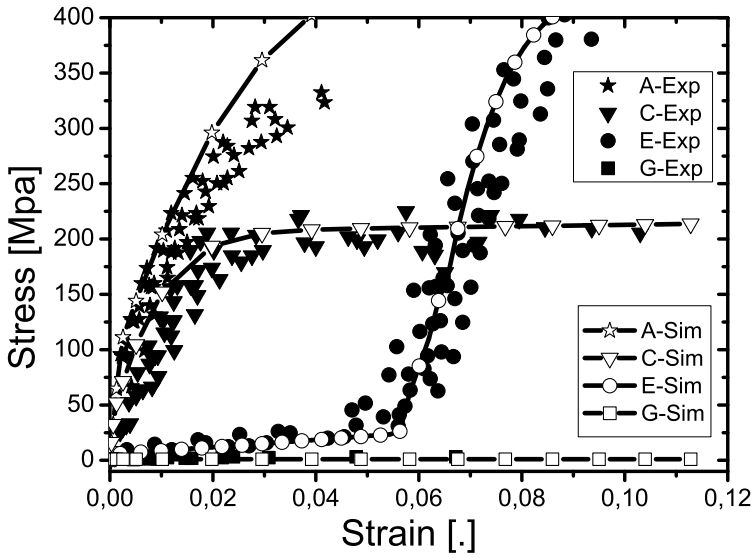

Figure 3: Comparison between experimental results reported by Kelley and Hosford (1968) and simulations for magnesium single crystals

8 Acknowledgement

The authors acknowledge the support of W. Hosford for providing the primary data of his pioneering experimental work on pure magnesium.

References

Agnew, S. R.; Duygulu, O.: A mechanistic understanding of the formability of magnesium: Examining the role of temperature on the deformation mechanisms. *Materials Science Forum*, 419-422, (2003), 177–188.

Agnew, S. R.; Yoo, M. H.; Tome, C. N.: Application of texture simulation to understanding mechanical behavior of mg and solid solution alloys containing li or y. *Acta Materialia*, 49, (2001), 4277–4289.

Ando, S.; Tonda, H.: Non-basal slip in magnesium-lithium alloy single crystals. *Material Transactions*, 41, (2000), 1188–1191.

Asaro, R. J.: Crystal plasticity. *Journal of Applied Mechanics*, 50, (1983), 921–934.

Bartels, S.; Carstensen, C.; Hackl, K.; Hoppe, U.: Effective relaxation for microstructure simulations: algorithms and applications. *Computer Methods in Applied Mechanics and Engineering*, 193, (2004), 5143–5175.

Beaudoin, A. J.; Dawson, P. R.; Mathur, K. K.; Kocks, U. F.: A hybrid finite element formulation for polycrystal plasticity with consideration of macrostructural and microstructural linking. *International Journal of Plasticity*, 11, (1995), 501–521.

Beausir, B.; Suwas, S.: Analysis of texture evolution in magnesium during equal channel angular extrusion. *Acta Materialia*, 56, (2008), 200–214.

Burke, E. C.; Hibbard, W. R.: Plastic deformation of magnesium single crystals. *Transactions of the Metallurgical Society of AIME*, 194, (1952), 295–303.

Carstensen, C.; Hackl, K.; Mielke, A.: Non-convex potentials and microstructures in finite-strain plasticity. *Proceeding of the Royal Society A*, 458, (2002), 299–317.

Coleman, B. D.: Thermodynamics of materials with memory. *Archive for Rational Mechanics and Analysis*, 17, (1964), 1–45.

Graff, S.; Brocks, W.; Steglich, D.: Yielding of magnesium: From single crystal to polycrystalline aggregates. *International Journal of Plasticity*, 23, (2007), 1957–1978.

Hauser, F. E.; Starr, C. D.; Tietz, L.; Dorn, J. E.: Deformation mechanisms in polycrystalline aggregates of magnesium. *Transactions of the ASM*, 47, (1955), 102–134.

Kelley, E. W.; Hosford, W. F.: Plane-strain compression of magnesium and magnesium alloy crystals. *Transactions of the Metallurgical Society of AIME*, 242, (1968), 654–661.

Kumar, A.; Dawson, P. R.: Modeling crystallographic texture evolution with finite elements over neo-eulerian orientation spaces. *Computer Methods in Applied Mechanics and Engineering*, 153, (1998), 259–302.

Lambrecht, M.; Miehe, C.; Dettmar, J.: Energy relaxation of non-convex incremental stress potentials in a strain-softening elastic-plastic bar. *International Journal of Solids and Structures*, 40, (2003), 1369–1391.

Lebensohn, R. A.; Tom, C. N.: A self-consistent anisotropic approach for the simulation of plastic deformation and texture development of polycrystals: application to zirconium alloys. *Acta Metallurgica et Materialia*, 41, (1993), 2611–2624.

Lee, E. H.: Elastic-plastic deformations at finite strains. *ASME, Journal of Applied Mechanics*, 36, (1969), 1–6.

Lubliner, J.: On the thermodynamic foundation of non-linear solid mechanics. *International Journal of Non-linear Mechanics*, 7, (1972), 237–254.

Lubliner, J.: *Plasticity Theory*. Maxwell Macmillian International Edition (1997).

Luenberger, D.: *Linear and Nonlinear Progrmming*. Addison-Wesley (1984).

Mandel, J.: *Plasticite Classique et Viscoplasticite*. Springer-Verlag (1972).

McGinty, R. D.; McDowell, D. L.: A semi-implicit integration scheme for rate independent finite crystal plasticity. *International Journal of Plasticity*, 22, (2006), 996–1025.

Miehe, C.; J. Schroeder, J.: A comparative study of stress update algorithms for rate-independent and rate-dependent crystal plasticity. *International Journal for Numerical Methods in Engineering*, 50, (2001), 273–298.

Mielke, A.: Deriving new evolution equations for microstructures via relaxation of variational incremental problems. *Computer Methods in Applied Mechanics and Engineering*, 193, (2004), 5095–5127.

Mosler, J.; Bruhns, O. T.: On the implementation of variational constitutive updates at finite strain. In: K. Hackl, ed., *Variational Concepts with Application to the Mechanics of Materials*, Springer (2009a), in press.

Mosler, J.; Bruhns, O. T.: Towards variational constitutive updates for non-associative plasticity models at finite strain: models based on a volumetric-deviatoric split. *International Journal of Solids and Structures*, 46, (2009b), 1676–1685.

Myagchilov, S.; Dawson, P. R.: Evolution of texture in aggregates of crystals exhibiting both slip and twinning. *Modeling and Simulation in Materials Science and Engineering*, 7, (1999), 975–1004.

Obara, T.; Yoshinga, H.; Morozumi, S.: {11-22} {-1-123} slip system in magnesium. *Acta Metallurgica*, 21, (1973), 845–853.

Ortiz, M.; Repetto, E. A.: Nonconvex energy minimization and dislocation structures in ductile single crystals. *Journal of the Mechanics and Physics of Solids*, 47, (1999), 397–462.

Ortiz, M.; Repetto, E. A.; Stainer, L.: A theory of subgrain dislocation structures. *Journal of the Mechanics and Physics of Solids*, 48, (2000), 2077–2114.

Ortiz, S. L., M.: The variational formulation of viscoplastic constitutive updates. *Computer Methods in Applied Mechanics and Engineering*, 171, (1999), 419–444.

Reed-Hill, R. E.; Robertson, W. D.: Additional modes of deformation twinning in magnesium. *Acta Metallurgica*, 5, (1957a), 717–727.

Reed-Hill, R. E.; Robertson, W. D.: Deformation of magnesium single crystals by nonbasal slip. *Journal of Metals - Transactions AIME*, 220, (1957b), 496–502.

Roberts, E.; Partridge, P. G.: The accomodation around {10-12} ¡-1011¿ twins in magnesium. *Acta Metallurgica*, 14, (1966), 513–527.

Schmid, E.: Yield point of crystals, critical shear stress law. In: *Proceedings of the First International Congress for Applied Mechanics, Delft* (1924).

Siebel, G.: *Magnesium und seine Legierungen*. Springer, Berlin (1939).

Simo, J. C.; Hughes, T. J. R.: *Computational Inelasticity*. Springer (1998).

Staroselsky, A.; Anand, L.: A constitutive model for hcp materials deforming by slip and twinning: application to magnesium alloy az31b. *International Journal of Plasticity*, 19, (2003), 1843–1864.

Tang, W.; Zhang, S.; Peng, Y.; Li, D.: Simulation of magnesium alloy az31 sheet during cylindrical cup drawing with rate independent crystal plasticity finite element method. *Computational Materials Science*, 46, (2009), 393–399.

Tegart, W. J. M.: Independent slip systems and ductility of hexagonal polycrystals. *Philosophical Magazine*, 9, (1964), 339–341.

Wonsiewicz, B. C.; Backofen, W. A.: Independent slip systems and ductility of hexagonal polycrystals. *Transaction of Metallurgical Soc. AIME*, 239, (1967), 1422–1433.

Yoshinaga, H.; Horiuchi, R.: On the nonbasal slip in magnesium crystals. *Transactions of the Japan Institute of Metals*, 5, (1963), 14–21.

Address: Malek Homayonifar, MSc., Prof. Dr.-Ing. habil. Joern Mosler, Institute of Materials Research, Materials Mechanics, GKSS Research Centre, D-21502 Geesthacht, Germany
email: malek.homayonifar@gkss.de, joern.mosler@gkss.de